Turkish Journal of Electrical Engineering & Computer Sciences

http://journals.tubitak.gov.tr/elektrik/

Research Article

Turk J Elec Eng & Comp Sci
(2020) 28: 2643 – 2656

doi:10.3906/elk-1912-45

Low-profile folded dipole UHF RFID tag antenna with outer strip lines for metal mounting application

Fuad ERMAN[1], Effariza HANAFI[1,*], Eng-Hock LIM[2], Wan Amirul WAN MOHD MAHYIDDIN[1], Sulaiman Wadi HARUN[1], Mohamad Sofian ABU TALIP[1], Rawan SOBOH[1], Hassan UMAIR[1]

[1]Department of Electrical Engineering, Faculty of Engineering, University of Malaya, Kuala Lumpur, Malaysia
[2]Department of Electrical and Electronic Engineering, Lee Kong Chian Faculty of Engineering and Science, University Tunku Abdul Rahman, Cheras, Malaysia

Received: 06.12.2019 • **Accepted/Published Online:** 15.04.2020 • **Final Version:** 25.09.2020

Abstract: A metal mountable UHF RFID tag antenna with a low-profile folded dipole structure is proposed. It is fabricated on a single layer of polytetrafluoroethylene (PTFE) dielectric laminate. It is composed of two symmetrical C-shape resonators integrated with the outer strip lines. The IC chip's terminals are connected directly to the center of the C-shaped resonators. The outer strip lines are integrated with the C-shaped resonators, which function to lower the reflection coefficient so as to match the IC chip impedance. In particular, the outer strip lines increase the inductive reactance of the antenna impedance in order to realize IC chip impedance. The design has a simple structure, due to the fact that it lacks any metallic vias. Moreover, the gain of the tag antenna can be enhanced when positioned on a large metallic sheet. Installed on a 40 × 40 cm^2 metallic plate, the total gain of the proposed tag antenna is 3 dB, with a maximum reading range of 5.77 m, while it is 3.92 m in free space. The simulation results were in excellent agreement with the fabricated design results.

Key words: Folded dipole, metal mountable tag antenna, high gain, impedance matching

1. Introduction

The implementation in the ultra-high frequency (UHF) band (860–960 MHz) of a passive radio frequency identification (RFID) tag is growing substantially due to its higher reading rate, enhanced reading range, and reduced tag size [1] relative to the low frequency (30–300 kHz) and high frequency bands (3-30 MHz) [2]. It is widely used in inventory systems, distribution logistics, retail sales, industries, and general detection systems [3–5]. A typical RFID system consists of several components: an RFID interrogator and an RFID tag antenna, which comprises an IC chip and an antenna [6]. The reading range of the tag antenna depends on its efficiency and gain and the minimum threshold power of the IC chip [7]. The circuit size, reading range, and compatibility of the tag antenna, with tagged objects, play a significant role in determining the performance of an antenna [8]. Trade-offs between gain, bandwidth, and overall size require careful and intricate manipulation of each element when designing a UHF tag antenna.

An RFID tag antenna designed for metallic objects with high gain, low reflection coefficient, and small size remains the most challenging task. Hence, mounting the tag antenna on a metallic object can affect the antenna's performance by decreasing the efficiency of an RFID tag. The majority of the applications that used

*Correspondence: effarizahanafi@um.edu.my

RFID tags as a part of them are made of metal. Consequently, it is important to design a tag antenna that can read near or on metallic surfaces by taking into account the effect of metallic surface conductivity on the antenna's performance. To overcome the deleterious effect of a metallic surface, several methods are being utilized to design a tag antenna with high performance. Electromagnetic bandgap (EBG) is applied by placing EBG cells around the antenna[9] or by etching the EBG ground surface with a lattice of circular slots [10]. Furthermore, the artificial magnetic conductor (AMC) method is implemented [11, 12] with offset vias, but the tag antenna is separated by an air gap or foam to prevent near field coupling with AMC substrate. The EBG structure and AMC approach increase the complexity of the design structure and cost significantly more due to the further work required. Other researchers proposed a single substrate tag antenna integrated with a reflector plane to enhance performance [13]; however, this made it bulky. In addition, applying various techniques such as the use of a thick substrate [14], implementation of parasitic elements [15], utilization of a parasitic substrate [16], separating the tag antenna from the metallic surface by foam or air foam [17, 18], inserting an air gap between two substrates [19], and employing a planar inverted-F antenna (PIFA) [20]; they improve the tag's performance, but the complexity of the structure and its fabrication and the overall cost increase to quite an extent. Therefore, in view of the above, the research and design of an RFID tag antenna suitable for mass production by being low profile, light weight, easy to fabricate, and low cost is still under exploration. We base this work on our previous simulations [21], which incorporated the use of split-ring resonators (SRRs). The analytical working principle of the tag antenna structure was not described there. Moreover, the performance enhancement with the use of SRRs was less than 0.5 dB in terms of gain. Herein we present in detail an improved folded dipole tag antenna design that is low profile and achieves better performance in terms of gain, read range, etc.

The function of the passive tag antenna is to efficiently retransmit power obtained from the reader. For that reason, it is essential that the tag antenna and microchip impedances are efficiently matched [22]. The input impedance of the microchip is usually designed with a low real part (3 to 150 Ω) and high negative imaginary part (–50 to –200 Ω). The input impedance of the tag antenna can be affected when mounted on various ground surfaces. Several techniques have been utilized for dipole antennas to match the capacitive reactance of IC chips, such as T-match [23], nested loop [24], and inductively coupled loop [25]. In Yang and Feng [26], a folded dipole tag antenna was presented with two circular loads, comprising an outer trace surrounding an inner circular part. The dimensions of these loads were designed to match the impedance of an IC chip. In Genovesi and Monorchio [27], an additional element was appended to the three-arm folded dipole antenna to fine tune the complex input impedance of the antenna. Two quarter-wavelength microstrip lines formed into meandered lines with stubs along with positioning the four shorting pins to realize impedance match were presented in Chen and Tsao [28]. Equilateral triangular stubs loaded to an S-shaped strip to accomplish the IC impedance was given in Ennasar et al. [17]. Adjusting the feed line of the modified dipole and meandered bar to precisely adjust the antenna's impedance was shown in Hamani et al. [19]. The tag antenna in Bong et al. [29] comprises a matching loop embedded into folded dipole arms incorporated with patches. The matching network of folded dipole in Benmessaoud et al. [13] comprises a loop included with a shorted stub and a pair of lines. A planar loop antenna loaded with two meandered line pairs realized the impedance matching with chip impedance by a miniaturized shunt-stub [30]. Therefore, in conclusion, designing an RFID tag antenna with a flexible design approach to conjugate match with any sort of IC chip is much desired.

In the present paper, a low-profile folded dipole tag antenna is proposed for metallic objects. It comprises two symmetrical C-shaped resonators with inductive outer strip lines mounted on each side of the tag chip and

are fed directly by the chip. The loaded outer strip lines increase the inductive reactance of the antenna to precisely realize the impedance of the IC chip. In contrast to previous works, the proposed design of the tag antenna is the least complex in its design to realize its resonance frequency and impedance match. Moreover, mounting the proposed design on metallic objects confirmed that increasing the dimensions of the metallic surface enhances the gain and reading range of the tag antenna. The achieved gain is higher than that reported in other works in the literature, despite the fact that it does not use any metallic vias or shorting stubs. The simulation results for the proposed method are confirmed with the results measured using the fabricated design.

2. Antenna structure

The folded dipole tag antenna with a low-profile structure is shown in Figure 1. The proposed tag antenna was fabricated on a low-cost polytetrafluoroethylene (PTFE) substrate with a thickness of 1.5 mm and a permittivity of 2.55 (loss tangent 0.0015). The proposed folded dipole tag antenna consists of two outer strip lines loaded on two symmetrical C-shaped resonators. One outer strip line is aligned with the upper horizontal part of the right arm of the folded dipole, connected to the upper left arm, while the second outer strip line is aligned with the lower horizontal part of the left arm of the folded dipole, connected to the lower right arm. The chip was attached between the C-shape resonators at the center of the layout.

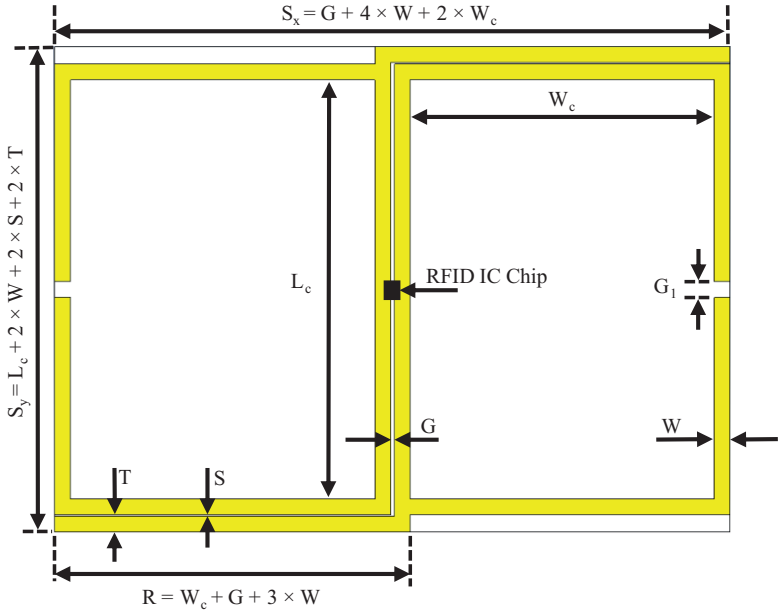

Figure 1. Geometry of the presented tag antenna S_y = 61.7, S_x = 86, W = T = 2, S = 0.2, G = 0.5, G_1 = 2, L_c = 53.3, W_c = 38.75 (unit: mm).

The midpoint of the symmetrical C-shaped resonators was directly connected to the terminals of the IC chip. Furthermore, outer strip lines were added to increase the inductance of the antenna to conjugate match the tag antenna's input impedance with that of the IC chip. The folded dipole antenna forms the input impedance network, where it can be easily optimized to realize the input impedance of any type of IC chip. This tuning of input impedance matching of the antenna can be precisely done by adjusting the width and length of the folded dipole antenna, making it operable at any UHF region band. The proposed design works in the North American band (902–928 MHz). The final dimensions of the presented tag antenna are shown in Figure 1, and it was attained by parametrically optimizing the length and width of the C-shape resonators.

3. Results and discussion

3.1. Parametric study

The full-wave electromagnetic simulator CST was used to analyze the performance of the designed RFID tag antenna. Its performance was tuned by mounting it on a square (200 mm side length) perfect electrical conductor (PEC), with 1 mm thickness. It is worth mentioning that there were no significant changes in tag antenna performance parameters when PEC thickness increased in terms of resonance frequency, reflection coefficient response, or obtained simulated gain. It utilized a Murata RFIDMAGICSTRAP LXMS31-ACNA-011 tag chip. The IC chip's input impedance usually comes with a low real part and high imaginary part. The utilized chip in the design has 25–j200 Ω impedance at its operating frequency of 915 MHz, with an −8 dBm RF threshold power.

The dimensions of the C-shape resonators must be carefully selected to realize a minimum reflection coefficient response. It is difficult to get the reflection coefficient response lower than −10 dB without the outer strip lines. It is regarded as the key to minimization of the S_{11} response. The outer strip lines work as inductors [31], increasing the inductance of the tag antenna at its input terminals and aiding in achieving a conjugate match to the IC chip impedance at the optimized dimension values. The input impedance of the outer strip line can be calculated from equation (5) in Lee et al. [32]. In other words, the presence of the outer strip lines intensifies the surface current in the folded dipole arms, thereby enhancing the antenna's inductance [33]. Further increasing the current paths would require adding strip lines on the outer sides. In the presence of outer strip lines, the surface current density of the tag antenna was increased from 233 A/m to 408 A/m, as shown in Figure 2. The length of these strip lines ($R = 3\times W + G + W_c$) is directly related to the C-shape resonators' width (W_c), as presented in Figure 1, which gives it a flexible tuning mechanism. The results of tuning the length of the C-shape (L_c) resonators are shown in Figure 3a, where it is regarded as the main factor in reducing the resonance frequency via varying the L_c length, shifting the resonance frequency down at a rate of 6 MHz/mm for a fixed W_c value. Each value of L_c has an associated W_c value in order for it to accomplish the ideal S_{11} response, as per Figure 3b. Varying W_c at a fixed L_c resulted in changes in the resonance frequency at the rate of 14 MHz/mm. Tuning the dimensions of the C-shape resonators via parametric analysis resulted in impedance matching.

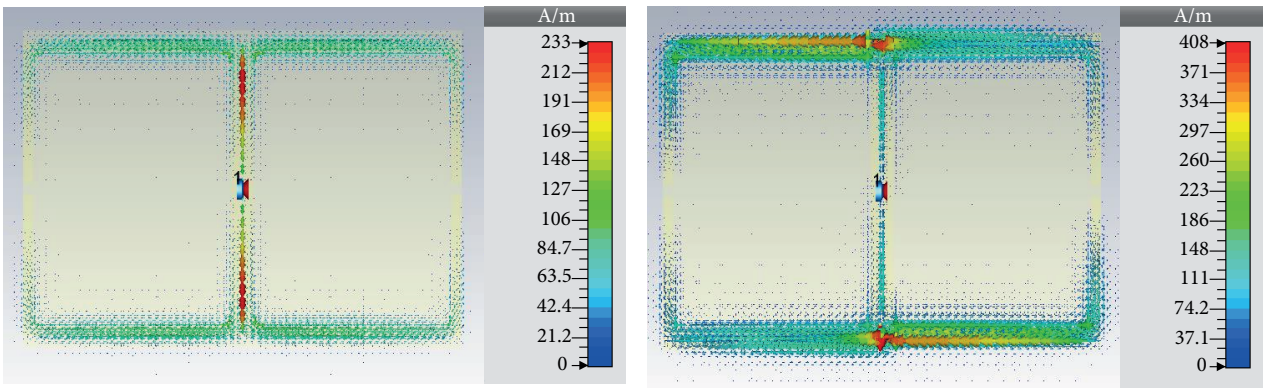

Figure 2. The surface current of the tag antenna (a) without outer strip lines (b) with outer strip lines.

The outer strip lines' presence emphasizes their role in minimizing the S_{11} response lower than −10 dB, by tuning the dimensions of the C-shape resonators with the existence of outer strip lines, as shown in Figure

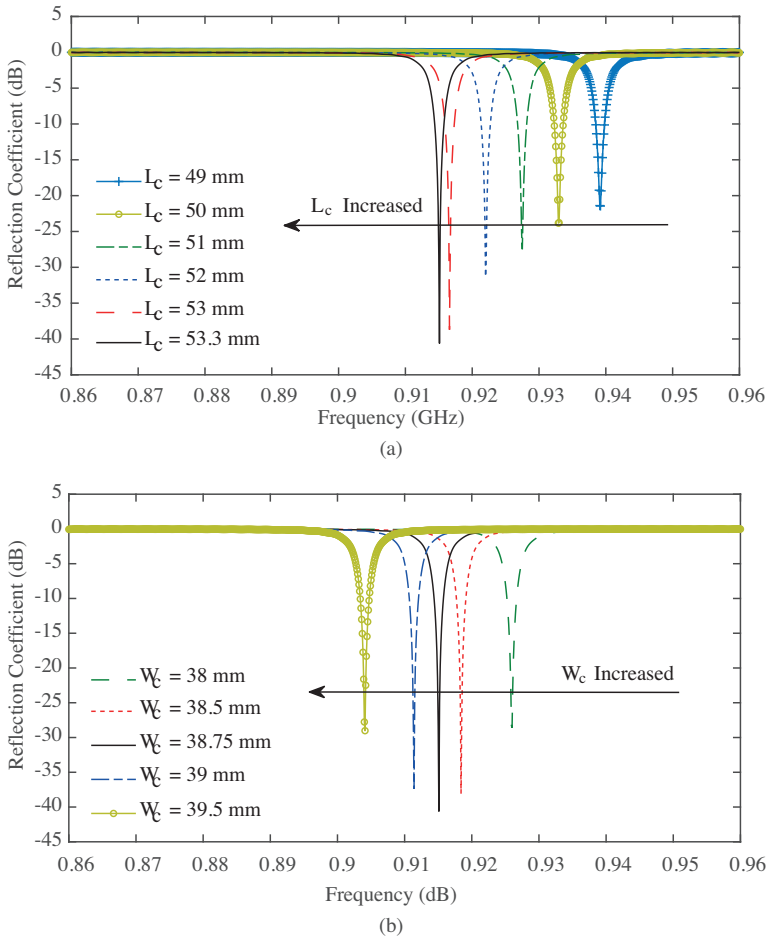

Figure 3. Simulated reflection coefficient response of the proposed design with outer strip lines: (a) various L_c values for fixed W_c = 38.75 mm and (b) various W_c values for fixed L_c = 53.3 mm.

3. This functionality resulted in attaining conjugate impedance matching with the IC chip. The tag antenna performance was investigated with and without outer strip lines in terms of its reflection coefficient response, as shown in Figures 3 and 4, respectively. After removing the outer strip lines, the C-shape resonators' dimensions were tuned to observe its effect on the reflection coefficient response. Figure 4 exhibited that achieving S_{11} response less than -10 dB is impossible without using outer strip lines. It can be seen in Figure 4a that the L_c values vary from 40 to 76 mm at fixed W_c = 38.75 mm. It can also be seen that although the S_{11} response shifts against the frequency axis at different L_c values, the minimum achieved S_{11} is not lower than -3 dB. Varying the value of W_c from 25 mm to 52 mm (at fixed L_c) resulted in a similar response, and as per Figure 4b, the S_{11} values do not exceed -3 dB over the entire range of varied W_c values. From Figures 4a and 4b, it can be inferred that for the proposed dimensions of the design the outer strip lines eased the attainability of impedance matching by lowering the S_{11} response to under -10 dB in the desired band.

The outer strip lines (R = 3 × W + G + W_c) were linked with the dimensions of the C-shape resonators to obtain the desired S_{11} response, where this part analyzes the impact of variations in outer strip lines' dimensions on S_{11} response, keeping the C-shaped resonator's dimensions fixed. This will help highlight the significance of outer strip lines. Figure 5a shows the length tuning of the outer strip lines (R), where it is evident that the best S_{11} response can be obtained once the length of the outer strip line is directly related

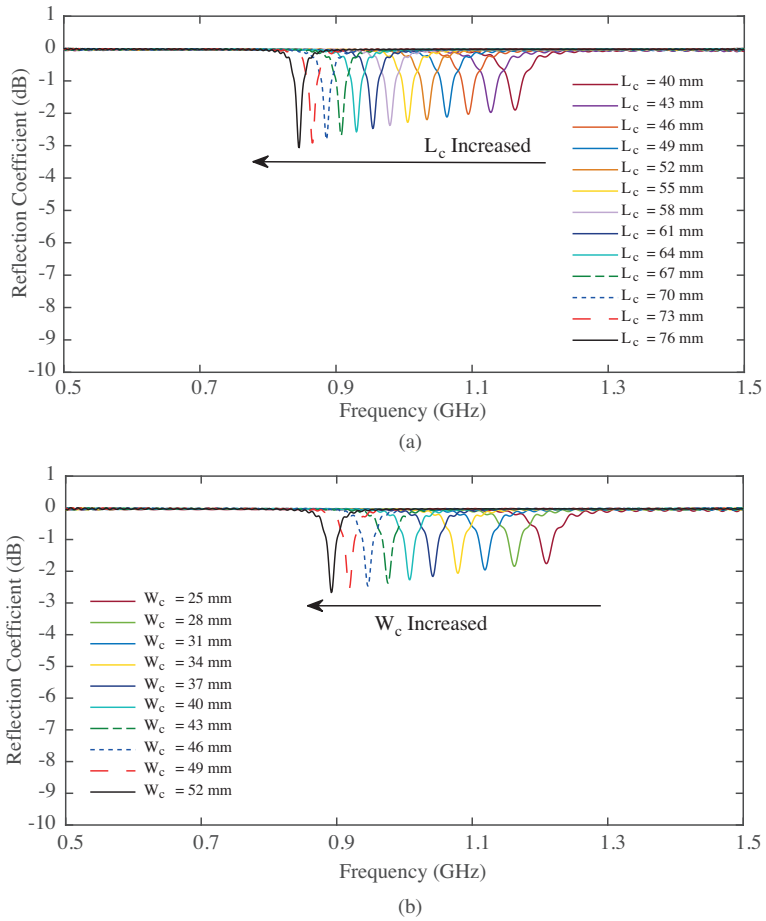

Figure 4. Simulated reflection coefficient response of the proposed design without outer strip lines: (a) various L_c values for fixed W_c = 38.75 mm and (b) various W_c values for fixed L_c = 53 mm.

to the width of the C-shaped resonator. It should also be pointed out that the width of outer strip line (T) was fixed while being tuned. Figure 5b shows the tuning of the width of the outer strip lines while keeping R associated with the C-shaped resonator width. It can be seen that once the dimensions of the outer strip lines are optimized as per the equation is given in Figure 1 (R linked to W_c, while T = W), we obtain the desired S_{11} response (below -10 dB) to realize impedance matching with the IC chip at its resonance frequency.

As the chip was attached to the mid-point between the C-shaped resonators, varying the dimensions of the C-shaped resonators had a profound impact on the conjugate input impedance presented to the IC chip. By varying the W_c of the C-shaped resonator in small increments, the variation in the antenna's resistance and reactance curves are shown in Figure 6. The variation in the reactance curves exceeded the variation in the resistance curves. The antenna impedance (25 + j206 Ω) is in excellent compliance with the tag IC impedance curves at its operating frequency of 915 MHz, and the reflection coefficient curves in Figure 3 are in agreement with the curves depicted in Figure 6.

3.2. Simulated and measured results

The measurement results of antenna input impedance, realized gain, detection distance, and read range pattern are presented in this section. The Voyantic Tagformance system was used to measure the reading distance,

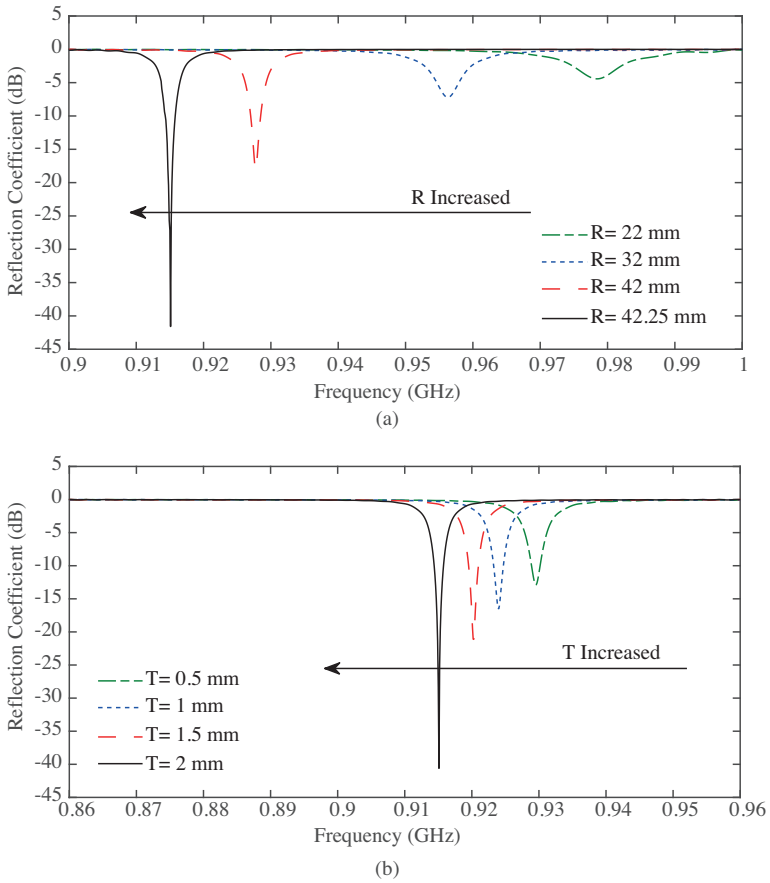

Figure 5. Simulated reflection coefficient response of the proposed design: (a) various R values for fixed T = 2 mm and (b) various R values for fixed R = 42.25 mm.

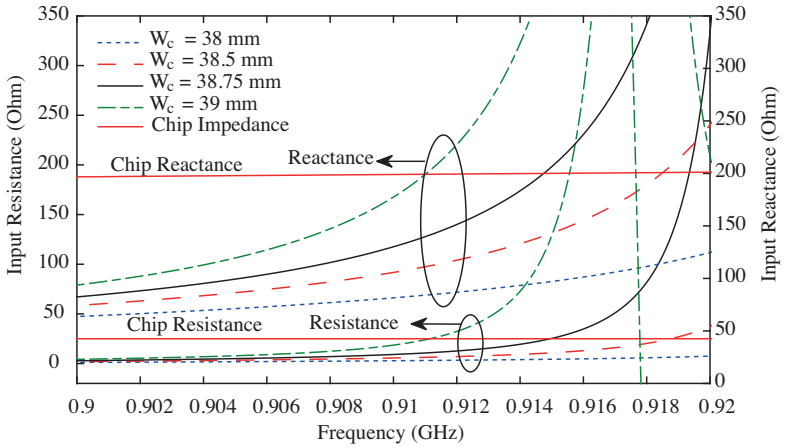

Figure 6. Simulated input resistance and reactance of the tag antenna for various W_c values.

realized gain, and read range pattern. The differential probe method was reported in Palmer and Van Rooyen [34] for measuring antenna input impedance. It was used because it is a practical and inexpensive technique, made up of two ports. The differential probe method involves measuring S-parameters to determine the input

resistance and reactance of the tag antenna. The differential probe is connected to a $37347D$ network analyzer on one side and to the fabricated design on the other side for the measurement.

The simulated antenna input impedance and measured antenna input impedance are plotted in Figure 7. It shows that there is a small variation between the simulated and measured reactance curves at the operating frequency, while the resistance curves are in excellent compliance with one another. These differences could be due to the soldering imperfections between the utilized probe and antenna, mismatch between the C-shaped resonators and SMA (SubMiniature version A) connectors, or defects from the fabrication processes.

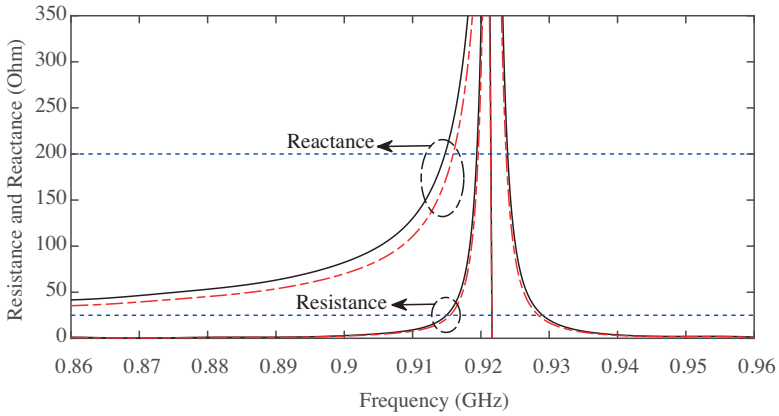

Figure 7. Simulated and measured input resistance and reactance of the proposed antenna design.

The tag antenna gain dictates the range of detection by the reader. The mounted folded tag antenna on a metallic object reported excellent gains. It can be observed that an increase in the metallic surface dimensions resulted in enhanced gain performance of the antenna. The simulated result of the gain is presented in Figure 8a for sheet sizes of 100, 200, 300, and 400 mm^2. The extension of the metallic sheet dimensions, from 100 mm^2 to 200 mm^2, increases the gain by $\sim$5.4 dB (from $-$3.3 dB at 100 mm^2 to 2.16 dB at 200 mm^2). The increase in the metallic sheet's size, from 200 mm^2 to 400 mm^2, enhances the gain by a further 1 dB. Henceforth, the achieved gain of the mounted design on the 400 mm^2 metallic plate at the center frequency (915 MHz) of the North American band (902–928 MHz) is 3 dB. However, the tag antenna impedance mismatch with the IC chip is included by the realized gain, G_r, as shown in Figure 8b, which can be calculated by equation (1). The simulated tag antenna G_r is $\sim$3 dB at 915 MHz, while its measured G_r is 1.65 dB at 917 MHz.

$$G_r = G_a \times \tau, \tag{1}$$

where G_a is the tag antenna gain.

Radiation efficiency is defined as the ratio of radiation power to input power. This is an important parameter of the tag antenna that is difficult to compute. The reduction in the antenna radiation efficiency can be caused by feeding network losses and surface wave excitation. Certain other factors can also affect the antenna efficiency significantly, such as fabrication tolerance effect, surface roughness, and spurious radiation, but the theoretical calculation does not take into account these losses. However, the calculation of losses is still possible to a certain extent. Three methods were reported for measurement of the antenna's efficiency, which are the gain/directivity method, Wheeler cap method, and radiometric method [35]. The gain/directivity method is the best known method for computing antenna efficiency. This method involves determining the gain, G, and

directivity, D_r, of the antenna. From this method, the computed antenna efficiency of the proposed tag is 35%, as given by the following equation:

$$\eta = P_{rad}/P_{in} = G/D_r, \tag{2}$$

where P_{rad} and P_{in} are the antenna radiated power and received power at the antenna's input terminal. The directivity of the proposed design is roughly constant (8.6 dBi) during the UHF band. Figure 8c shows the directivity and radiation efficiency of the tag antenna.

The reading range measurements of the tag antenna were made in an anechoic chamber by placing the tag on metallic sheets measuring 400 mm^2. In this condition, the detection distance (r) of the tag antenna by the reader exceeded 2 m and 2.5 m for 902–928 MHz and 905–926 MHz, respectively. The distance of 0.5 m was set between the tag antenna and reader, shown as the inset of Figure 9a. The employed RFID reader had 4 W of EIRP. The Friis formula was used to compute the antenna's detection distance over UHF band frequencies. The measured r was verified with computed results as shown in Figure 9a. The calculated r for a 400 mm^2 sheet was 5.77 m, while in the free space it was 3.92 m. The measured maximum r on the 400 mm^2 metallic sheet was up to 5 m at the center frequency of 917 MHz. The discrepancy between the measured and calculated r was $\sim$13%.

The read range is used to depict the radiation characterization via graphical presentation. The read pattern of the tag antenna presents the response of the tag to the reader as exhibited in Figures 9b and 9c. The distance between the tag and the reader was kept fixed through the entire measurements, while the tag was rotated around the y-, x-, and z-axis for depicting the read range pattern in the xz, yz, and xy planes. The detection distance beyond $\theta = \mp 90^0$ was truncated because the metallic surface functioned as a reflector, while the maximum measured read range of the proposed tag in the boresight direction ($\theta = 0$) was 5 m. In Figure 9d, the simulated radiation patterns of the proposed design at 915 MHz, when it was placed on a PEC sheet of 400×400 mm^2, are depicted for the xz and yz principal planes.

Table 1 compares the proposed tag antenna with other metal-mountable tag antennas. A fair comparison is achieved by recomputing the detection distance using a constant threshold power ($P_{ic} = -18.5$ dBm) and a fixed reader power (EIRP = 4 W). The tag in Kamalvand et al. [9] used electromagnetic band gap (EBG) unit cells around the antenna to reduce the surface wave propagation and side lobe radiation. This method significantly enhanced the gain and reading range, but it also required 52 vias and shorting pins to be shorted to the ground. In Kim and Yeo [12] the AMC substrate with offset vias was separated by an air gap from the tag antenna, which increased the complexity and size. The RFID tag antenna in Bilgiç and Yeğen [14] has a one-layer structure, with a 2.73 dB peak gain, but the thickness of the design is 3.175 mm. SRRs are utilized in Lee et al. [15] to conjugate match the chip impedance and improve radiation efficiency, while two shorting stubs are used for bringing the resonance frequency down. Its thickness exceeds 2 mm, which is not preferable for metallic applications. In addition, a parasitic substrate composed of semicircular dipolar patches is utilized in Niew et al. [16] for matching purpose. It is loaded orthogonally on top of identical pair patches with shorting stubs, forming a dual layer tag antenna with thickness exceeding 2 mm. Elsewhere [17, 18], single layer tag antennas are separated from metallic surface by foam (1 cm thickness) and air foam (1.5 mm thickness), respectively. Two FR4 layers, each 0.8 mm thick and separated by an air gap, with 7.6 mm of total tag thickness were presented in Hamani et al. [19]. That method also uses plastic screws to maintain a fixed air gap between the FR4 layers. The fabrication process is complex and costly due to the presence of multiple layers of substrate, vias, shorting pin, and plastic screws. The RFID tag antenna in Yang and Son [20] consists

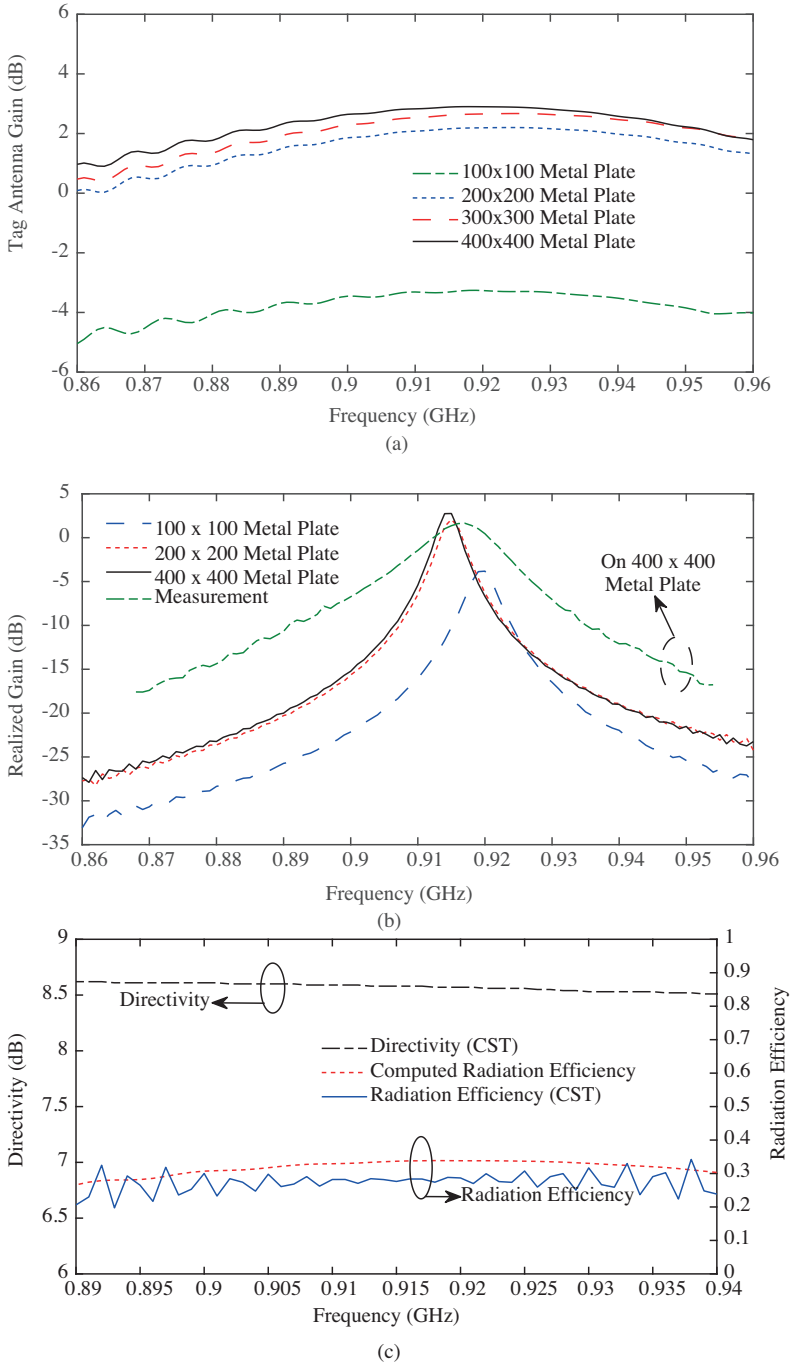

Figure 8. (a) Simulated gain and (b) simulated and measured realized gain of the presented RFID tag antenna mounted on various metal plates sizes, (c) the directivity and radiation efficiency of the proposed tag antenna.

of two PIFA antennas, having 12 vias included in its structure. Our proposed low-profile design is of a simple structure, and in contrast to the compared works it does not incorporate any complexity in terms of its design technique (like AMC/EBG) or design geometry (like vias/gaps/parasitic elements), and the design can be easily fabricated on a single PTFE-layer. In addition, our proposed design also can achieve a higher degree of gain.

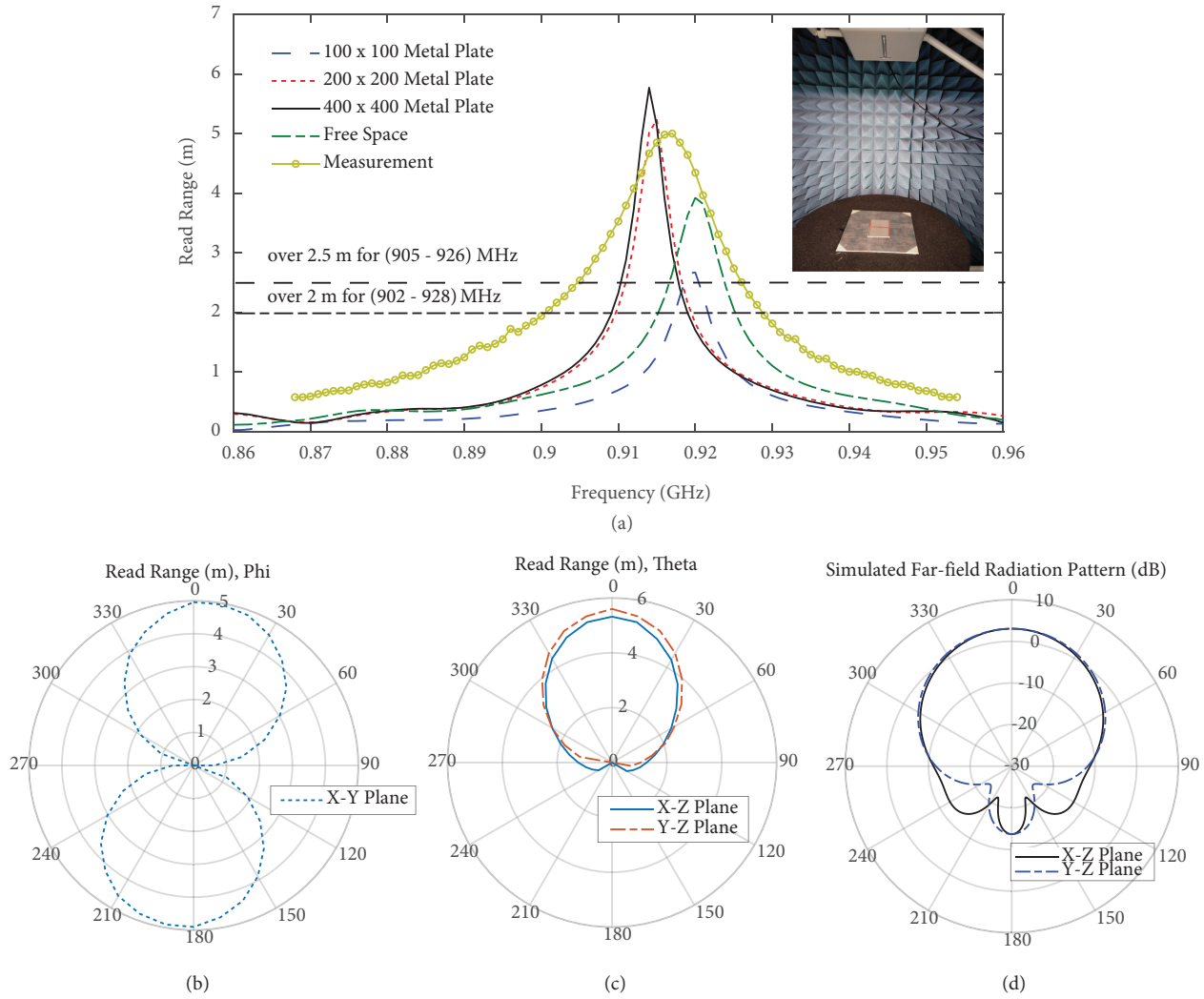

Figure 9. (a) The computed and measured read range for the proposed design, measured read range pattern for (b) xy, (c) yz and xz planes at 917 MHz, (d) simulated far-field radiation pattern at 915 MHz for the designed tag antenna mounted on 400×400 mm^2 PEC surface.

Furthermore, the MURATA chip has a high level of threshold power relative to Higgs (Alien Technology) or Monza (Impinj); therefore, replacing the chip could improve the read range threefold.

4. Conclusion

The suggested RFID tag antenna has been successfully designed to be implemented on metallic objects. Moreover, the folded tag antenna structure accommodates the flexible method for tuning complex impedance and resonance frequency, which do not require shorting stubs or metallic vias. The fabrication process is rather cheap. The dimensions of the folded dipole can be easily optimized to realize the input impedance of the chip after the addition of the inductive outer strip lines. Its gain was 3 dB, due to the mounting of the tag antenna on a 400×400 mm^2 metallic plate. This design is regarded as a good candidate for RFID implementation attached to metallic surfaces.

Table . Comparison table between UHF metal mountable tags.

Ref.	Tag Dimension (mm)	Substrate	P_{ic} (dBm)	G_r (dB)	r (m)	Normalized r (m)	Bandwidth (MHz)
[9]	70×70×1.6	FR4	-	-9	6.1	4.93	-
[11]	100×60×10	FR4+Air	-17	0.377	12.2	14.5	-
[14]	94×94×3.175	Taconic-RF43	-	2.73	-	19.01	-
[15]	40×40×3.18	PET+Foam	-17.8	-2.21	9.5	10.765	-
[16]	40×40×3.05	RO4003C	-18.5	-1.27	12.25	12.25	-
[17]	57×43×11.58	FR4+Foam	-8	0.115	4.2	14.07	28
[18]	120×60×1.9	FR4+Air Foam	-18	4.41	10	23.07	10
[19]	104×31×7.6	FR4+Air	-8.5	2.1	14.6	17.68	153
[20]	64×64×2	FR4	-17.4	-1.18	10.2	12.12	-
Proposed	86×61.7×1.5	PTFE	-8	3	5.77	19.61	12

Acknowledgments

This work was supported in part by the University of Malaya Research University Grant-Faculty Programme under Grant No. GPF027A-2019 and in part by University of Malaya Faculty Research Grant under Grant No. GPF029A-2018.

References

[1] Bansal A, Sharma S, Khanna R. Compact meandered RFID tag antenna with high read range for UHF band applications. International Journal of RF and Microwave Computer-Aided Engineering 2019; 29 (11): e21695. doi: 10.1002/mmce.21695

[2] Liu G, Xu L, Wu Z. Miniaturized circularly polarized microstrip RFID antenna using fractal metamaterial. International Journal of Antennas and Propagation 2013; 2013: 1-4. doi: 10.1155/2013/781357

[3] Erman F, Hanafi E, Lim EH, Mahyiddin WM, Harun SW et al. Miniature compact folded dipole for metal mountable UHF RFID tag antenna. Electronics 2019; 8 (6): 713. doi: 10.3390/electronics8060713

[4] Calis G, Becerik-Gerber B, Göktepe AB, Shuai LI, Nan LI. Analysis of the variability of RSSI values for active RFID-based indoor applications. Turkish Journal of Engineering & Environmental Sciences 2013; 37 (2): 186-210. doi: 10.3906/muh-1208-3

[5] Sevinc Y, Kaya A. Reconfigurable antenna structure for RFID system applications using varactor-loading technique. Turkish Journal of Electrical Engineering & Computer Sciences 2012; 20 (4): 453-462. doi: 10.3906/elk-1004-519

[6] Al-Azzawi BF, Rigelsford JM, Langley RJ. Investigations into improving the detectability of self-resonant RFID tags. IET Microwaves, Antennas & Propagation 2018; 12 (9): 1519-1525. doi: 10.1049/iet-map.2017.1205

[7] Salman KN, Ismail A, Abdullah RSAR, Saeedi T. Coplanar UHF RFID tag antenna with U-shaped inductively coupled feed for metallic applications. PLoS One 2017; 12 (6): e0178388. doi: 10.1371/journal.pone.0178388

[8] Siakavara K, Goudos S, Theopoulos A, Sahalos J. Passive UHF RFID tags with specific printed antennas for dielectric and metallic objects applications. Radioengineering 2017; 26 (3): 735-745. doi: 10.13164/re.2017.0735

[9] Kamalvand P, Kumar Pandey G, Kumar Meshram M, Mallahzadeh A. A single sided dual-antenna structure for UHF RFID tag applications. International Journal of RF and Microwave Computer-Aided Engineering 2015; 25 (7): 619-628. doi: 10.1002/mmce.20900

[10] Ukkonen L, Sydanheimo L, Kivikoski M. Effects of metallic plate size on the performance of microstrip patch-type tag antennas for passive RFID. IEEE Antennas and Wireless Propagation Letters 2005; 4: 410-413. doi: 10.1109/LAWP.2005.860212

[11] Park IY, Kim D. Artificial magnetic conductor loaded long-range passive RFID tag antenna mountable on metallic objects. Electronics Letters 2014; 50 (5): 335-336. doi: 10.1049/el.2013.2671

[12] Kim D, Yeo J. Low-profile RFID tag antenna using compact AMC substrate for metallic objects. IEEE Antennas and Wireless Propagation Letters 2008; 7: 718-720. doi: 10.1109/LAWP.2008.2000813

[13] Benmessaoud L, Vuong TP, Yagoub MC, Touhami R. A novel 3-D tag with improved read range for UHF RFID localization applications. IEEE Antennas and Wireless Propagation Letters 2017; 16: 161-164. doi: 10.1109/LAWP.2016.2565378

[14] Bilgic MM, YEĞİN K. An HF/UHF dual mode RFID transponder antenna and HF range extension using UHF wireless power transmission. Turkish Journal of Electrical Engineering & Computer Sciences 2016; 24 (5): 3949-3960. doi: 10.3906/elk-1412-169

[15] Lee YH, Lim EH, Bong FL, Chung BK. Bowtie-shaped folded patch antenna with split ring resonators for UHF RFID tag design. IEEE Transactions on Antennas and Propagation 2019; 67 (6): 4212-4217. doi: 10.1109/TAP.2019.2908268

[16] Niew YH, Lee KY, Lim EH, Bong FL, Chung BK. Patch-loaded semicircular dipolar antenna for metal-mountable UHF RFID tag design. IEEE Transactions on Antennas and Propagation 2019; 67 (7): 4330-4338. doi: 10.1109/TAP.2019.2905675.

[17] Ennasar MA, Aznabet I, EL Mrabet O, Essaaidi M. Design and characterization of a compact single layer modified S-shaped tag antenna for UHF-RFID applications. Advanced Electromagnetics 2019; 8 (1): 59-65. doi: 10.7716/aem.v8i1.845

[18] Lin YF, Chang MJ, Chen HM, Lai BY. Gain enhancement of ground radiation antenna for RFID tag mounted on metallic plane. IEEE Transactions on Antennas and Propagation 2016; 64 (4): 1193-1200. doi: 10.1109/TAP.2016.2526047

[19] Hamani A, Yagoub MCE, Vuong TP, Touhami R. A novel broadband antenna design for UHF RFID tags on metallic surface environments. IEEE Antennas and Wireless Propagation Letters 2017; 16: 91-94. doi: 10.1109/LAWP.2016.2557778

[20] Yang ES, Son HW. Dual-polarised metal-mountable UHF RFID tag antenna for polarisation diversity. Electronics Letters 2016; 52 (7): 496-498. doi: 10.1049/el.2016.0076

[21] Erman F, Ismail A, Abdullah RSAR, Alhawari ARH, Shabaneh A et al. UHF RFID split ring resonator-based tag antenna with photonic bandgap structure for metallic objects. Journal of Fundamental and Applied Sciences 2017; 9 (3S): 630-636. doi: 10.4314/jfas.v9i3s.49

[22] Alhawari ARH, Ismail A, Jalal ASA, Abudullah RSAR, Rasid MFA. U-shaped inductively coupled feed radio frequency identification tag antennas for gain enhancement. Electromagnetics 2014; 34 (6): 487-496. doi: 10.1080/02726343.2014.922767

[23] Pumpoung T, Phongcharoenpanich C. Design of wideband tag antenna for ultra-high-frequency radio frequency identification system using modified T-match and meander-line techniques. Electromagnetics 2015; 35 (5): 340-354. doi: 10.1080/02726343.2015.1043851

[24] Balanis CA. Antenna Theory: Analysis and Design. Hoboken, NJ, USA: John Willey & Sons, 1997.

[25] Son HW, Pyo CS. Design of RFID tag antennas using an inductively coupled feed. Electronics Letters 2005; 41 (18): 994-996. doi: 10.1049/el:20051536

[26] Yang B, Feng Q. A folded dipole antenna for RFID tag. In: 2008 International Conference on Microwave and Millimeter Wave Technology; Nanjing, China; 2008. pp. 1047-1049.

[27] Genovesi S, Monorchio A. Low-profile three-arm folded dipole antenna for UHF band RFID tags mountable on metallic objects. IEEE Antennas and Wireless Propagation Letters 2010; 9: 1225-1228. doi: 10.1109/LAWP.2010.2103295

[28] Chen HD, Tsao YH. Low-profile PIFA array antennas for UHF band RFID tags mountable on metallic objects. IEEE Transactions on Antennas and Propagation 2010; 58 (4): 1087-1092. doi: 10.1109/TAP.2010.2041158

[29] Bong FL, Lim EH, Lo FL. Compact folded dipole with embedded matching loop for universal tag applications. IEEE Transactions on Antennas and Propagation 2017; 65 (5): 2173-2181. doi: 10.1109/TAP.2017.2676776

[30] Gao X, Shen Z. UHF/UWB tag antenna of circular polarization. IEEE Transactions on Antennas and Propagation 2016; 64 (9): 3794-3802. doi: 10.1109/TAP.2016.2583547.

[31] Greenhouse HM. Design of planar rectangular microelectronic inductors. IEEE Transactions on Parts, Hybrids and Packaging 1974; 10 (2): 101-109. doi: 10.1109/TPHP.1974.1134841

[32] Lee SR, Lim EH, Bong FL, Chung BK. Slotted circular patch with multiple loading stubs for platform insensitive tag. IEEE Transactions on Antennas and Propagation 2018; 66 (10): 5072-5079. doi: 10.1109/TAP.2018.2858149

[33] Ng WH, Lim EH, Bong FL, Chung BK. Folded patch antenna with tunable inductive slots and stubs for UHF tag design. IEEE Transactions on Antennas and Propagation 2018; 66 (6): 2799-2806. doi: 10.1109/TAP.2018.2821702.

[34] Palmer KD, van Rooyen MW. Simple broadband measurements of balanced loads using a network analyze. IEEE Transactions on Instrumentation and Measurement 2006; 55 (1): 266-272. doi: 10.1109/TIM.2005.861493

[35] Pozar DM, Kaufman B. Comparison of three methods for the measurement of printed antenna efficiency. IEEE Transactions on Antennas and Propagation 1988; 36 (1): 136-139. doi: 10.1109/8.1084